Taylor & Francis
Taylor & Francis Group

Electric Power Components and Systems

ISSN: 1532-5008 (Print) 1532-5016 (Online) Journal homepage: www.tandfonline.com/journals/uemp20

S-transform-based Hybrid Active Filter for Mitigation of Current Harmonics

C. Venkatesh, D. V. S. S. Siva Sarma & M. Sydulu

To cite this article: C. Venkatesh, D. V. S. S. Siva Sarma & M. Sydulu (2009) S-transform-based Hybrid Active Filter for Mitigation of Current Harmonics, Electric Power Components and Systems, 37:12, 1305-1320, DOI: 10.1080/15325000903054977

To link to this article: https://doi.org/10.1080/15325000903054977

Published online: 18 Nov 2009.

Electric Power Components and Systems, 37:1305–1320, 2009

ISSN: 1532-5008 print/1532-5016 online
DOI: 10.1080/15325000903054977

Taylor & Francis
Taylor & Francis Group

S-transform-based Hybrid Active Filter for Mitigation of Current Harmonics

C. VENKATESH,[1] D. V. S. S. SIVA SARMA,[1] and M. SYDULU[1]

[1]Electrical Engineering Department, National Institute of Technology, Warangal, India

Abstract *This article presents a new control strategy for the hybrid active filter using S-transform. Frequency-domain analysis employing S-transform is used to extract the fundamental component of the non-linear load current. The switching patterns for the active filter are generated with pulse-width modulation. The proposed technique is simple and has better performance, even with low switching frequency, as compared to time-domain techniques. Simulation results are presented for steady-state and transient conditions, and the hybrid active filter is effective in maintaining the source current harmonics within the limits.*

Keywords active filters, current harmonics, power quality, S-transform

1. Introduction

In anticipation of the proliferation of non-linear loads and to limit the problems caused by harmonic currents, the IEEE-519 [l] guidelines are used, which specify the allowable harmonic distortion in the currents drawn from the utility system. Various types of current harmonic filters, such as passive filters, shunt active filters [2–5], series active filters [6–8], and hybrid filters [9–13], are used for the purpose of limiting utility current distortion.

Two fundamental approaches that are employed in the control circuit of active filters are correction in the time domain and correction in the frequency domain. Early designs of current harmonic compensators are based on the time-domain approach; pulse-width modulation (PWM)-based methods, such as constant frequency control [4, 14], hysteresis control [3, 6–8], and triangular wave control [15–17], were used to control the switches in the active filters. The advantage of time-domain methods is the fast response for on-line applications without complicated control circuitry. This advantage occurs because time-domain control strategies operate on instantaneous values of the distorted waveform rather than at least one period of data as in frequency-domain methods; thus, the required computational time can be relatively small. The shortcoming of time-domain methods is that, in order to obtain optimum results, relatively high switching frequencies are needed, which subsequently leads to excessive switching losses in the semiconductor switches. The frequency-domain correction approach [18–20] first uses Fourier analysis of the

Received 29 August 2008; accepted 13 April 2009.
Address correspondence to Mr. C. Venkatesh, Electrical Engineering Department, National Institute of Technology, Warangal, Andhra Pradesh, 506 004, India. E-mail: challacvs@ieee.org

distorted waveform to determine the required compensation current needed to correct the distorted waveform, and then it determines the switching pattern of a converter used to produce a close approximation to the compensation current.

Frequency-domain methods include predetermined harmonic injection [18] and PWM-based techniques such as the optimized injection method [19] and adaptive frequency control [20]. Switching frequencies for frequency-domain methods can be much lower than in time-domain schemes, resulting in lower semiconductor switching losses. Many conventional frequency-domain control approaches have been developed. Recently, the wavelet transform [20–22] technique has been employed to extract the harmonic components of the signal. Wavelet transform with multi-resolution analysis [23] used to decompose the signal into multiple levels of detail and approximation coefficients gives information on a band of frequencies but cannot identify a particular frequency and also fails to provide phase information of the harmonics.

S-transform (ST) is an extension of wavelet transform or a variable-window short-time Fourier transform. A key feature of ST [24] is that it uniquely combines a frequency-dependent resolution of the time-frequency space and absolutely referenced local phase information. The phase correction of the wavelet transform in the form of ST can provide significant improvement in the detection and localization of power quality disturbance transients [25–27]. Classification of power quality disturbances with ST is gaining more importance due to its ability to classify the disturbances accurately with no further requirement of other pattern classifiers such as neural networks or fuzzy logic.

In this article, a novel control technique for mitigation of source current harmonics is proposed by using ST as a tool to generate the reference current signal for active filter operation. Each module of the hybrid active filter is discussed in detail. The performance of this filter under steady-state and transient conditions are presented by means of simulation results.

2. System Configuration and Principle of Operation

The block diagram of the proposed hybrid filter system for mitigation of source current harmonics is shown in Figure 1. It consists of an active filter connected in series with the supply and a passive filter in shunt with the load. The shunt passive filter suppresses the harmonic currents produced by the load, whereas the series active filter acts as a harmonic isolator between the source and the load.

The active filter is a voltage source PWM-based power electronic converter. Figure 2 shows the operating principle of the filter on per-phase base. Here, the active filter is represented as a controllable voltage source v_{AF}, and the load is considered as current source i_{load}. The equivalent impedance of the shunt passive filter is represented as Z_{PF} and the source impedance as Z_S. The series active filter is controlled in such a way as to present zero impedance to the external circuit at the fundamental frequency and a high resistance K to the source harmonics or load harmonics. Figure 2 gives two equivalent circuits, as shown in Figures 3(a) and 3(b), at the fundamental frequency f_1 (= 50 Hz) and at harmonic frequency f_h ($= hf_1$), respectively.

At the fundamental frequency, the active filter in Figure 3(a) allows a current $\overline{I}_{S_1} = \overline{I}_{load_1} + \overline{I}_{PF_1}$ to flow through it, where the fundamental current $\overline{I}_{PF_1}$ is drawn by the passive filter network and $\overline{I}_{load_1}$ is the fundamental load current.

At a harmonic frequency f_h, the active filter in Figure 3(b) acts like an isolator, forcing all of the load harmonic current ($\overline{I}_{load_h}$) to flow through the passive filter network. The voltage across the passive filter ($\overline{V}_{PF_h}$) and the voltage across the active filter ($\overline{V}_{AF_h}$)

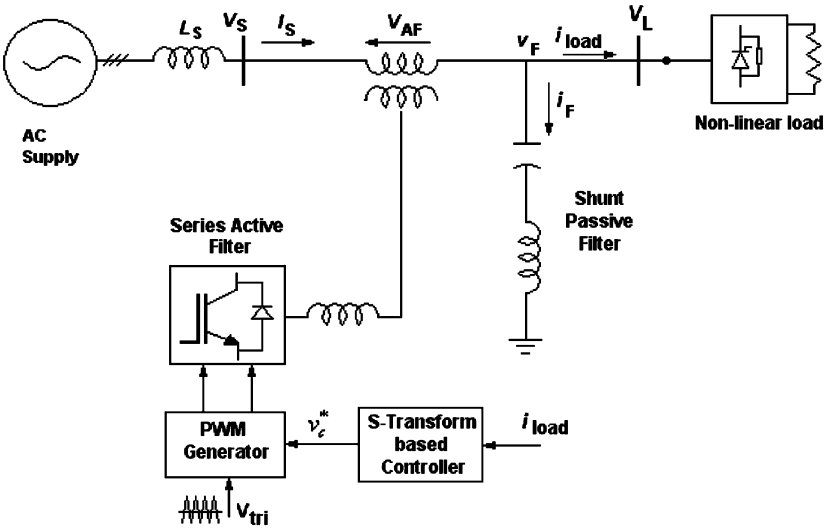

Figure 1. Combination of series active filter and shunt passive filter for current harmonics mitigation.

at harmonic frequency f_h are given by Eqs. (1)–(3) as

$$\overline{V}_{PF_h} = Z_{PF_h}.\overline{I}_{load_h} \tag{1}$$

and

$$\overline{V}_{AF_h} = K.\overline{I}_{S_h} = K\frac{Z_{PF_h}.\overline{I}_{load_h} + \overline{V}_{S_h}}{Z_{S_h} + Z_{PF_h} + K}, \tag{2}$$

where Z_{PF_h} and Z_{S_h} are the passive filter impedance and the source impedance at frequency f_h, respectively, and $\overline{V}_{S_h}$ is the source voltage at frequency f_h.

If $K \gg |Z_{PF_h}|, |Z_{S_h}|$, then Eq. (2) can be written as

$$\overline{V}_{AF_h} \cong Z_{PF_h}.\overline{I}_{load_h} + \overline{V}_{S_h}. \tag{3}$$

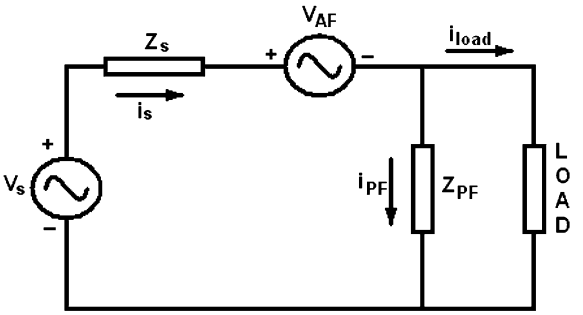

Figure 2. Equivalent circuit of the system of Figure 1 on per-phase base.

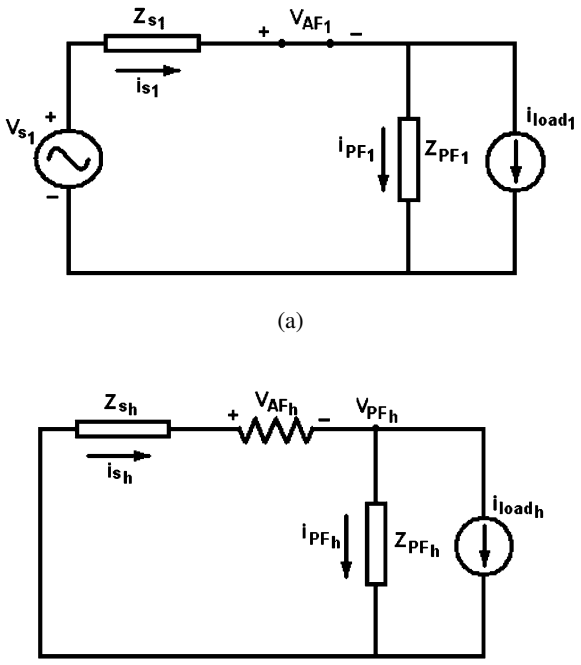

Figure 3. Equivalent circuit: (a) for fundamental frequency and (b) for harmonic frequencies.

If the resistance K is much larger than the source impedance, variations in the source impedance have no effect on the filtering characteristics of the shunt passive filter, thus reducing the source harmonic current to zero.

The rating of the active filter is given as

$$VA_{AF} = \overline{V}_{AF}.\overline{I}_S. \tag{4}$$

2.1. Control Strategy

To control the series active filter in such a way as to present zero impedance for the fundamental frequency and pure resistance for the harmonics, the reference output voltage of the series active filter [9] is constructed as

$$v_c^* = K.i_{ref}^*, \tag{5}$$

where i_{ref}^* is the source harmonic current to be compensated. This i_{ref}^* is obtained as

$$i_{ref}^* = i_{load} - i_{load,1}, \tag{6}$$

where i_{load} is the load current, and $i_{load,1}$ is the fundamental component of load current. The ST-based controller shown in Figure 1 is proposed in this article to extract $i_{load,1}$ from the measured load current.

3. ST

ST can be seen as the "phase correction" of continuous wavelet transform (CWT). The CWT of function $h(t)$is defined as

$$W(\tau, d) = \int_{-\infty}^{\infty} h(t).w(d, t-\tau).dt, \tag{7}$$

where d is the scale parameter that determines the width of the wavelet $w(d, \tau)$, and τ is the translation factor.

The ST of the function $h(t)$ is defined as the CWT with a specific mother wavelet multiplied by the phase factor and is given by

$$S(\tau, f) = e^{-j2\pi ft}.W(\tau, d), \tag{8}$$

where the mother wavelet is defined as

$$w(t, f) = \frac{|f|}{\sqrt{2\pi}}.e^{-\frac{t^2 f^2}{2}}.e^{-j2\pi ft}. \tag{9}$$

The wavelet in Eq. (9) does not satisfy the condition of zero mean for an admissible wavelet; therefore, Eq. (8) is not strictly a CWT. Written out explicitly, ST is defined as

$$S(\tau, f) = \int_{-\infty}^{\infty} h(t).\frac{|f|}{\sqrt{2\pi}}.e^{-\frac{(\tau-t)^2 f^2}{2}}.e^{-j2\pi ft}dt. \tag{10}$$

ST can also be written as operations on the Fourier spectrum $H(f)$ of $h(t)$ as

$$S(\tau, f) = \int_{-\infty}^{\infty} H(\alpha + f).e^{-\frac{2\pi^2\alpha^2}{f^2}}.e^{-j2\pi\alpha\tau}.d\alpha, \qquad f \neq 0. \tag{11}$$

The signal $h(t)$ can be expressed in a discrete form as $h(kT)$ for $k = 1, \ldots, N$, where T is the sampling time interval and N is the total sampling number. For $\tau \to kT$ and $f \to n/NT$, the ST of a discrete time series is given by

$$S\left[kT, \frac{n}{NT}\right] = \sum_{m=0}^{N-1} H\left[\frac{m+n}{NT}\right].e^{-\frac{2\pi^2 m^2}{n^2}}.e^{\frac{j2\pi mk}{N}}, \tag{12}$$

for $n \neq 0$ and where $k, m = 1, \ldots, N$ and $n = 1, \ldots, N$.

Equation (12) represents a time-frequency representation of a time series in the form of a complex valued ST-matrix (STC matrix). Each row of the STC matrix gives the particular frequency component of the signal analyzed at various sampling times. Each column of the STC matrix represents the magnitude and phase angles of the harmonic components in the signal at a given time or sample. It uniquely combines a frequency-dependent resolution that simultaneously localizes the real and imaginary spectra. With the advantage of fast lossless invariability from time domain to time-frequency domain and back to the time domain, the usage of ST is very analogous to the Fourier transform. The STC matrix generates contours that are suitable for classification by simple visual

inspection, unlike wavelet transform that requires specific methods like standard-deviation multi-resolution analysis [23].

The one-dimensional function of the variable τ and fixed parameter f_1 defined by $S(\tau, f_1)$ is called a voice of f_1, written as

$$S(\tau, f_1) = A(\tau, f_1).e^{-\varphi(\tau, f_1)}, \tag{13}$$

where $A(\tau, f_1) = |S(\tau, f_1)|$ is the amplitude, and $\varphi(\tau, f_1) = \arctan(\mathrm{Im}[S(\tau, f_1)]/\mathrm{Re}[S(\tau, f_1)])$ is the phase of the voice.

The linear property of ST insures that, for the case of additive harmonics (where one can model the data as $signal(t) = fundamental(t) + harmonics(t)$), the ST gives $S\{signal\} = S\{fundamental\} + S\{harmonics\}$. Thus, it will be easier to identify the fundamental and harmonics of the signal.

4. Extraction of Fundamental and Current Harmonics Using ST

This section shows the application of ST in extracting the harmonics contained in the current signal. Figures 4(a)–6(a) are current signals considered for analysis, which are generated using a MATLAB code with a known value of harmonic signal combined with the fundamental value. The sampling frequency considered is 2 kHz. ST analysis can extract the information of these harmonics along with magnitude and phase angle.

Figure 4(a) is a stationary signal consisting of 1 p.u. of the fundamental signal within phase (1/3) p.u. of the third harmonic. Harmonic analysis of this signal is performed by formulating the STC matrix using ST. Figure 4(b) shows the plot of RMS value (in p.u.) of the signal versus samples. The RMS values are obtained from the STC matrix by

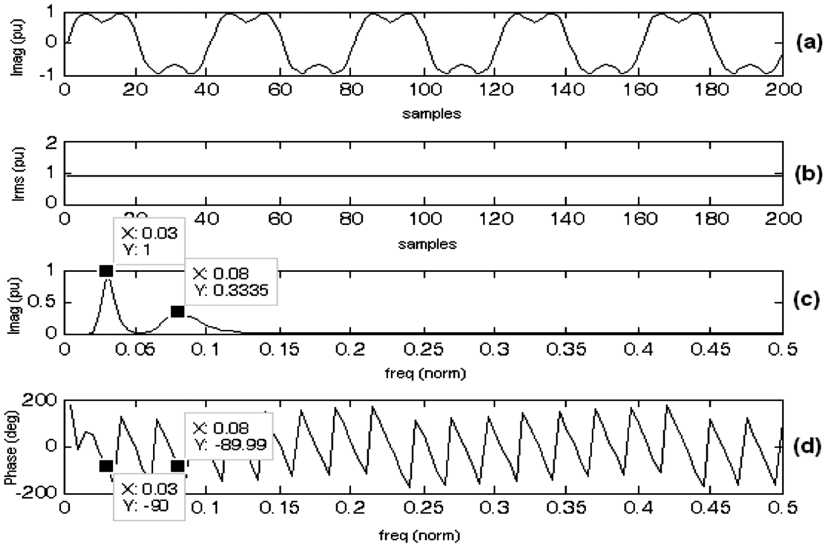

Figure 4. Current waveform with fundamental and third harmonic.

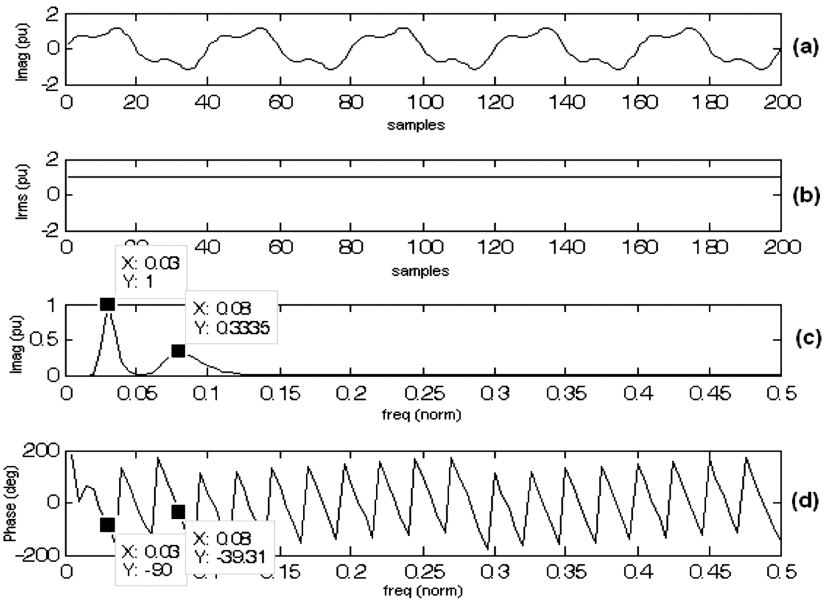

Figure 5. Current waveform with fundamental and third harmonic with phase shift.

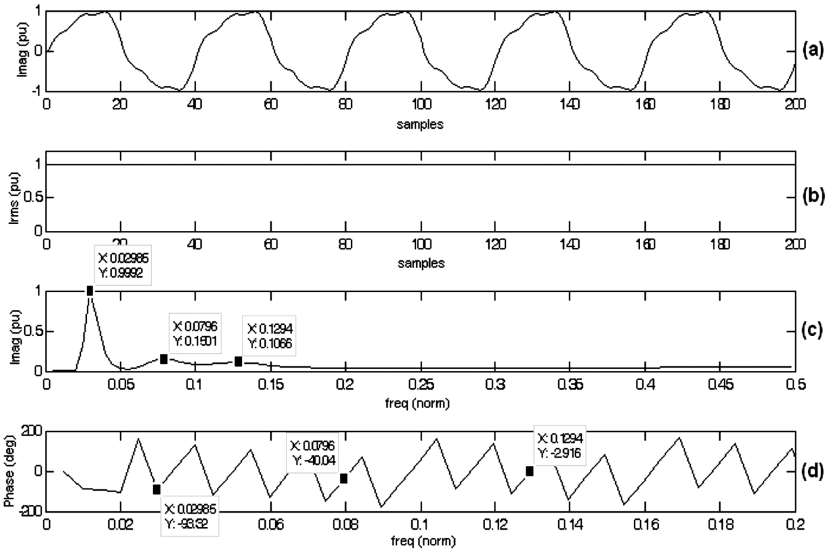

Figure 6. Current waveform with fundamental, third and fifth harmonics.

Table 1
Extraction of current harmonics using ST

	Simulated signal frequency components			ST solution of frequency components			
Signal	Freq. (Hz)	Mag. (p.u.)	Phase (°)	Norm. freq.	Mag. (p.u.)	Phase (°)	Phase diff. (°)
Figure 4(a)	50	1.00	0	0.03	1.00	−90	In phase
	150	0.33	0	0.08	0.3335	−89.99	
Figure 5(a)	50	1.00	0	0.03	1.00	−90	50.69
	150	0.33	50	0.08	0.3335	−39.31	
Figure 6(a)	50	1.00	0	0.03	0.9992	−90	49.96 and 87.08
	150	0.15	50	0.08	0.1501	−40.04	
	250	0.10	87	0.13	0.1066	−2.916	

identifying the maximum amplitudes of the signal at every sample using

$$\max(|S[kT, n/NT]|), \tag{14}$$

where $k = 1, 2, \ldots, N$ and $n = 1, 2, \ldots, (N/2)$.

Figure 4(c) is the normalized frequency curve. Peak values on this curve occur at dominant frequencies. The X and Y coordinate values indicated in Figure 4(c) gives the normalized frequency and RMS value of the signal (in p.u.), respectively, at the peak values of the normalized frequency curve. Normalized frequency (f_n) is given by

$$f_n = \frac{n.f_1}{f_s}, \tag{15}$$

where $n = 1, 2, \ldots, (N/2)$, f_1 is the fundamental frequency (50 Hz), and f_s is the sampling frequency (2 kHz). The phase angles of all the frequency contents at a particular time can be obtained from the STC matrix.

Figure 4(d) shows the curves of normalized frequency versus the phase angle calculated from the STC matrix at all rows of a column. The X and Y coordinate values indicated in Figure 4(d) are the normalized frequency and phase angles, respectively, for the dominant frequencies indicated in Figure 4(c).

ST analysis is also performed for other cases of harmonic content in the current signal. Figure 5(a) is the fundamental signal of 1 p.u. containing (1/3) p.u. of the third harmonic with a phase difference of 50°. Figure 6(a) is a stationary signal with 1 p.u. fundamental, (1/3) p.u. third harmonic, and (1/5) p.u. fifth harmonic components. Figures 5(b)–5(d) and 6(b)–6(d) show the plots obtained from ST analysis. Table 1 summarizes the simulation results of ST harmonic analysis. From the table it is clear that by using ST, harmonics in the current can be easily identified. This feature of ST is used to design the controller for the hybrid active filter.

5. Simulation Model of the Proposed System

The MATLAB/Simulink model of the proposed ST-based hybrid filter is shown in Figure 7. The passive filter is designed for the major harmonics such as the third, fifth and

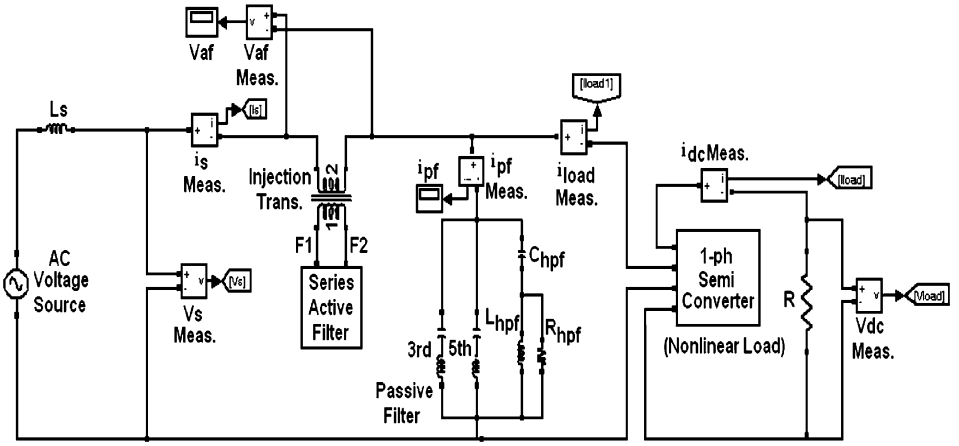

Figure 7. MATLAB/Simulink model of the ST-based hybrid filter.

a high-pass filter (HPF) for the eleventh harmonic. The design values of the filter and load specification are given in Table 2. The series active filter is modeled with a single-phase full-bridge inverter as shown in Figure 8.

The PWM generator block of Figure 8 consists of ST-based harmonic current extraction as shown in Figure 9. The load current (i_{load}) is sensed, and a MATLAB code is used to perform ST analysis of this signal. From the STC matrix constructed for i_{load}, information, such as the peak value and phase angle of the fundamental component ($i_{load,1}$), are extracted. The reference current signal i^*_{ref} is then calculated as ($i_{load} - i_{load,1}$), and it represents the harmonic components of the load current. To control the series active

Table 2
System parameters used for simulation of hybrid active filter

	Supply
RMS voltage	230 V
Frequency	50 Hz
Source impedance	L_S
	Shunt passive filter
For third harmonic	$L = 3.26$ mH, $C = 340$ μF
For fifth harmonic	$L = 1.2$ mH, $C = 340$ μF
HPF	$L = 0.26$ mH, $C = 300$ μF, $R = 3$ Ω
	Series active filter
DC bus voltage	220 V
PWM frequency	2 kHz
Ripple filter	$L = 10$ mH, $C = 57$ μF
	Load
One-phase full-bridge converter	230 V, 6 kW with resistive load, $R_1 = 10$ Ω

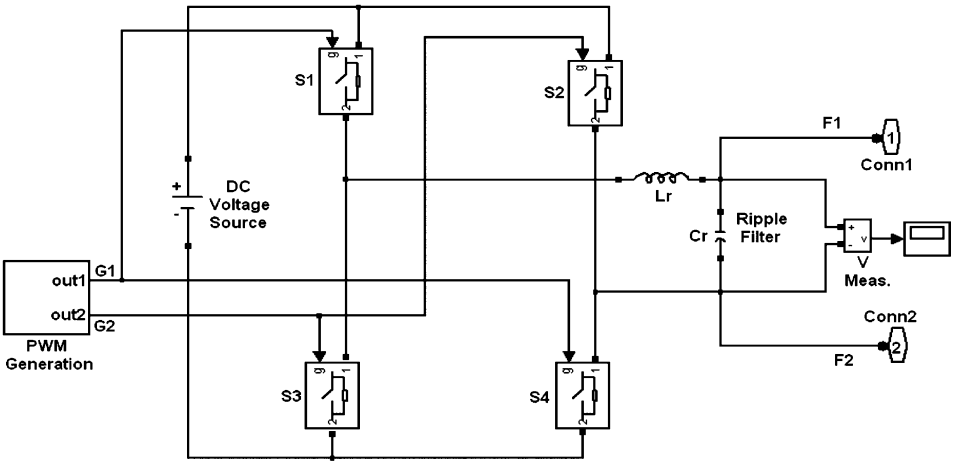

Figure 8. Series active filter model.

filter in such a way as to present zero impedance for the fundamental and pure resistance for the harmonics, the reference output voltage of the series active filter is calculated from i^*_{ref} as given by Eq. (5). Gate pulses are generated by the PWM technique as shown in Figure 9.

6. Simulation Results

Simulation analysis is first performed for the non-linear load of single-phase controlled rectifier with a resistive load of $R = 10\ \Omega$ and without the hybrid filter. The waveforms of supply voltage v_s, source current i_s, load current i_{load} on the AC side of the converter load, and DC current i_{dc} in resistance R for this case are shown in Figure 10. The source current in Figure 10(b) is discontinuous, and the total harmonic distortion (THD) of the source current is found to be 15.08%. When the proposed hybrid filter is introduced, as in Figure 7, ST analysis is performed for the load current in Figure 10(b). The variation of magnitudes and phase angles of the fundamental and harmonic components

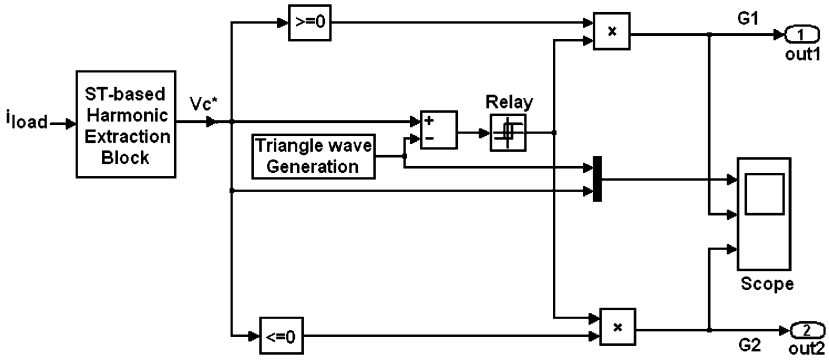

Figure 9. Control voltage and gate pulse generation.

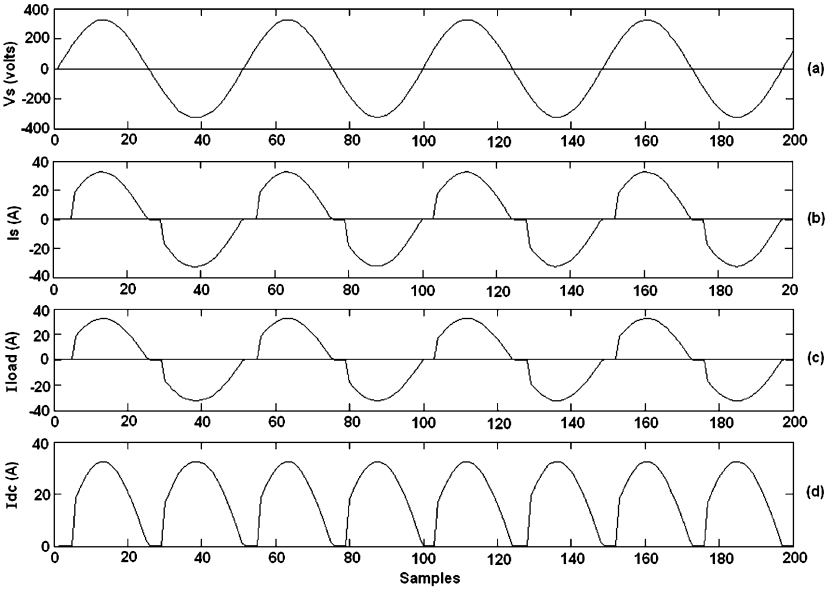

Figure 10. Waveforms of supply voltage, source current, load current on AC side of the converter load, and current in resistive load $R = 10\ \Omega$ (without filter).

present in the load current are extracted, and the corresponding frequency-magnitude and frequency-phase plots are shown in Figures 11(a) and 11(b), respectively.

The fundamental load current $i_{load,1}$, shown in Figure 12(a), is constructed from the magnitude and phase angle information obtained from ST analysis. The reference current signal in Figure 12(b) is obtained by the ST harmonic extraction block. Through the injected voltage generated by the voltage source indicator (VSI), the active filter is

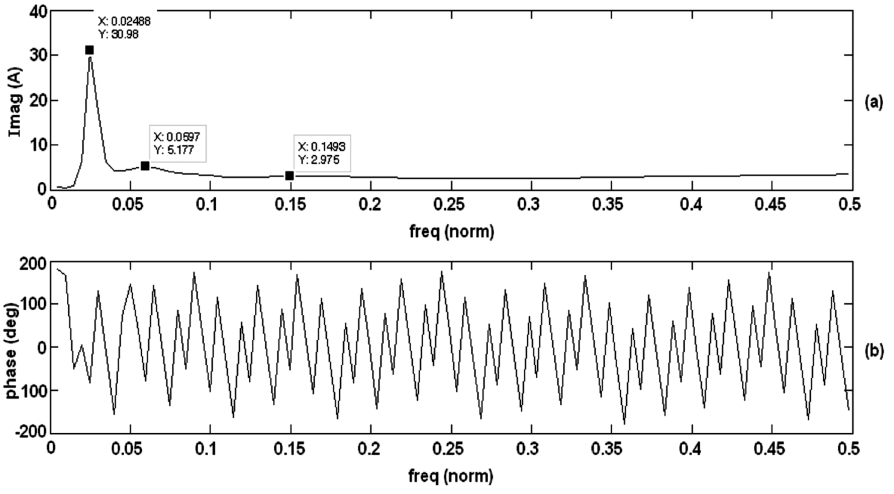

Figure 11. Fundamental and harmonic extraction of load current by ST.

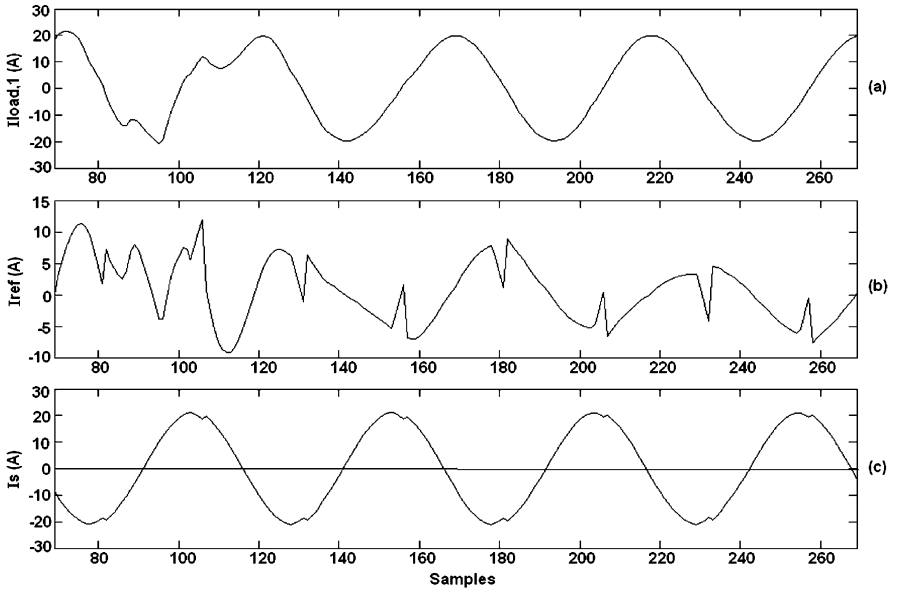

Figure 12. Current waveforms with ST-based hybrid active filter (HAF): (a) fundamental component of load current $i_{load,1}$, (b) reference current i^*_{ref}, and (c) source current i_s.

able to compensate for most of the harmonics in the source current. The source current is approximately sinusoidal, and the THD is now 1.982%.

Simulation results of dominant harmonic magnitudes in the source and load currents are given in Table 3. The harmonic spectrum of i_s in Figure 13 shows the performance of the proposed ST-based hybrid active filter in maintaining the source current harmonics within the limits as per the IEEE Std. 519 specifications. Performance of the filter is tested for rectifier with R load, RL load, and RC loads. The THDs of the source current and load current are given in Table 4 for these loads. The computer load consists of four computers that are modeled in MATLAB/Simulink.

Figure 14 shows the simulation result when four computers are connected as load. The personal computer (PC) is a highly non-linear load, which draws a current shown in Figure 14(a) having a THD of 91.4%. A typical PC load model uses switch-mode power supply (SMPS) and comprises of a full-wave rectifier, a DC storage capacitor, a diode bridge resistance, and a series radio frequency interference (RFI) choke. A PC model

Table 3
Percentage of harmonics and THD of load and source currents

	Load current I_{load} (%)				Source current I_s (%)			
Filter	$h = 3$	$h = 5$	$h = 7$	THD	$h = 3$	$h = 5$	$h = 7$	THD
Without filter	8.15	7.19	5.19	15.08	8.15	7.19	5.19	15.08
ST-based hybrid filter	3.79	4.29	4.04	10.38	0.72	0.81	0.77	1.982

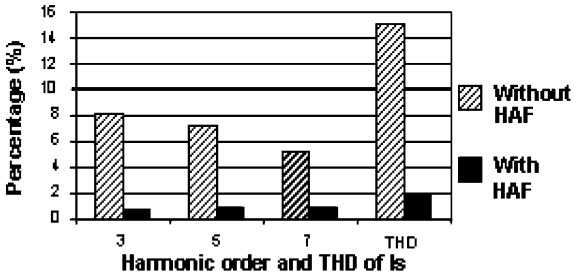

Figure 13. Harmonic spectrum of source current for without and with ST-based HAF.

developed in MATLAB/Simulink is validated by comparing the source current obtained from simulation with the practical computer current. The fundamental component of this current and the reference current for the active filter are shown in Figures 14(b) and 14(c), respectively. The series active filter injects the control voltage given in Figure 14(d), which supplies the harmonic current, and hence, fundamental current is drawn from the supply, as shown in Figure 14(e). The source current THD is 1.73%.

The dynamic performance of the filter is tested with a change in load from 20 Ω to 10 Ω at 0.08 sec. The filter could trace the change in load current and inject suitable harmonic current to make the source current sinusoidal. The waveforms of load current and source current are shown in Figures 15(a) and 15(b), respectively. The filter compensates the harmonics in the source current at 0.1 sec, and hence, the control circuit takes one cycle to perform ST analysis and generate the reference current signal. Variation of the THDs of load current and source current are shown in Figure 15(c).

Simulation is also performed to test the filter for various source inductances. Table 5 shows the effect of source inductance on the source voltage. With the increase in source inductance, the source voltage harmonics increase. The ST-based hybrid active filter brings the THD of the source current to less than 5% and the source voltage THD less than 2%. Hence, the proposed ST-based hybrid active filter is effective in operating and compensating the utility current harmonics.

Table 4
THD percent of load and source currents with ST-based HAF

Load connected at the controlled rectifier output	I_{load} (% THD)	I_s (% THD)
$R = 10$ ohms	15.08	1.98
$R = 15$ ohms	15.07	2.55
$R = 20$ ohms	15.12	1.93
$R = 20$ ohms $+L = 10$ mH	11.23	1.44
$R = 20$ ohms $+L = 30$ mH	11.32	1.38
$R = 20$ ohms $+C = 10$ μF	11.44	0.004
$R = 20$ ohms $+C = 1$ μF	9.36	0.003

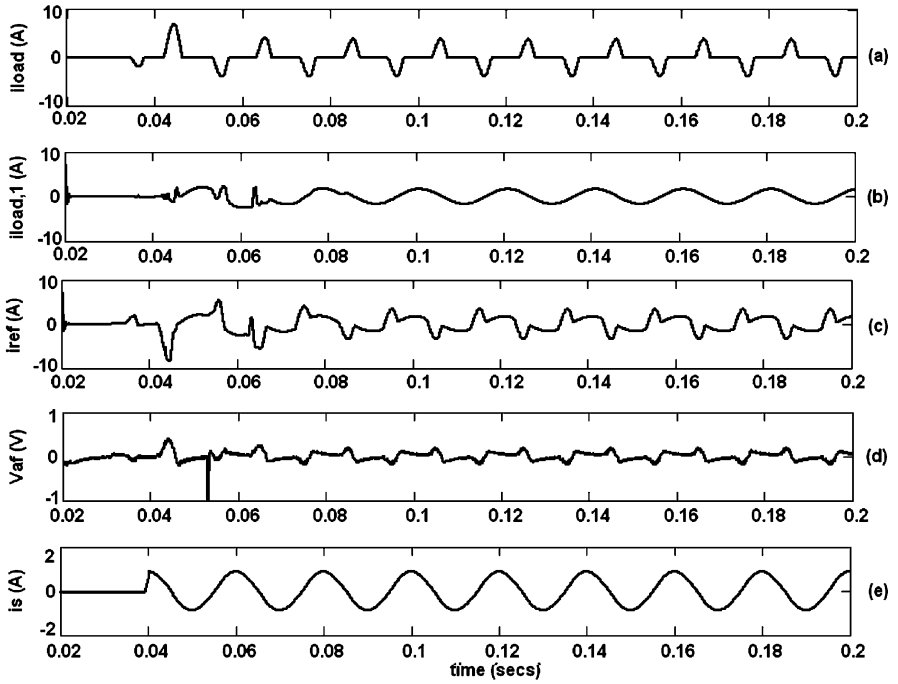

Figure 14. Simulation for computer load with STbased HAF: (a) load current drawn by computer, (b) fundamental component of load current, (c) reference current, (d) voltage injected by series active filter, and (e) source current.

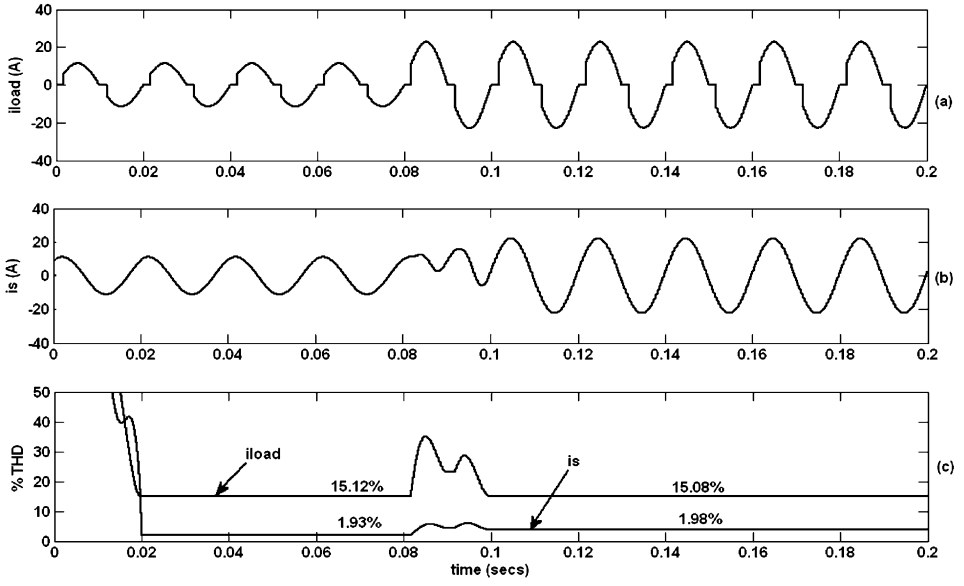

Figure 15. Performance of ST-based HAF for change in load from 20 Ω to 10 Ω at 0.08 sec: (a) load current, (b) source current, and (c) %THD curves for the load and source currents.

Table 5
Performance of ST-based hybrid filter for various source impedances

Source inductance L_S (mH)	Load current I_{load} (amp)	Filter	THD (%)	
			Source current I_s (amp)	Source voltage V_S (volts)
0	15.08	Without filter	15.08	0
		With filter	1.98	0
0.5	14.65	Without filter	14.65	3.50
		With filter	3.35	0.77
0.75	14.43	Without filter	14.43	4.29
		With filter	1.75	0.76
1.0	14.22	Without filter	14.22	4.97
		With filter	3.35	1.24

7. Conclusion

This article proposes a new control technique for the series active filter employing ST for reference signal generation. The proposed filter is able to maintain the source current harmonics within the limits for various non-linear loads under steady-state and transient conditions. The operation of the proposed hybrid filter is found to be satisfactory when tested for different source impedances.

References

1. "IEEE recommended practices and requirements for harmonic control in electrical power systems," IEEE Std. 519, 1992.
2. Aredes, M., and Monteiro, L. F. C., "A control strategy for shunt active filter," *10th Int. Conf. Harmonics Quality Power*, Vol. 2, pp. 472–477, 2002.
3. Tey, L. H., So, P. L., and Chu, Y. C., "Improvement of power quality using adaptive shunt active filter," *IEEE Trans. Power Delivery*, Vol. 20, No. 2, pp. 1558–1568, April 2005.
4. Duke, R. M., "The steady-state performance of a controlled current active filter," *IEEE Trans. Power Electron.*, Vol. 8, pp. 140–146, April 1993.
5. Akagi, H., Nabae, A., and Atoh, S., "Control strategy of active power filters using multiple voltage-source PWM converters," *IEEE Trans. Ind. Appl.*, Vol. IA-22, pp. 460–465, May/June 1986.
6. Chiang, H.-K., Lin, B.-R., and Wu, K.-W., "Series active power filter for current harmonic and load voltage compensation," *IEEE Region 10 International Conference 2005*, Melbourne, Australia, 21–24 November 2005.
7. Singh, B., and Verma, V., "A new control scheme of series active filter for varying rectifier loads," *Fifth Int. Conf. Power Electron. Drive Syst. (PEDS 2003)*, Vol. 1, pp. 554–559, November 2003.
8. Antchev, M., Gurgulitsov, V., and Petkova, M., "Study of PWM and sliding-mode controls implied to series active power filters," *50th Int. Symp. (ELMAR-2008)*, Vol. 2, pp. 419–422, 10–12 September 2008.
9. Peng, F. Z., Akagi, H., and Nabae, A., "A new approach to harmonic compensation in power systems—a combined system of shunt passive and series active filters," *IEEE Trans. Ind. Appl.*, Vol. 26, No. 6, pp. 554–559, November/December 1990.

10. Akagi, H., "Active harmonic filters," *Proc. IEEE*, Vol. 93, No. 12, pp. 2128–2140, December 2005.
11. Fujita, H., and Akagi, H., "A practical approach to harmonic compensation in power systems—series connection of passive and active filters," *IEEE Trans. Ind. Appl.*, Vol. 27, No. 6, pp. 1020–1025, November/December 1991.
12. Rastogi, M., Mohan, N., and Edris, A.-A., "Hybrid-active filtering of harmonic currents in power systems," *IEEE Trans. Power Delivery*, Vol. 10, No. 4, pp. 1994–2000, October 1995.
13. Barbosa, P. G., Santisteban, J. A., and Watanabe, E. H., "Shunt-series active power filter for rectifiers AC and DC sides," *Proc. Elect. Power Appl.*, Vol. 145, No. 6, pp. 577–584, November 1998.
14. Mohan, N., "A novel approach to minimize line-current harmonics in the interfacing power electronics equipment with three-phase utility systems," *IEEE Trans. Power Delivery*, Vol. 8, pp. 1395–1401, July 1993.
15. Morán, L. A., Dixon, J. W., and Wallace, R. R., "A three-phase active power filter operating with fixed switching frequency for reactive power and current harmonic compensation," *IEEE Trans. Ind. Electron.*, Vol. 42, pp. 402–408, August 1995.
16. Dixon, J. W., Garcia, J. J., and Moran, L., "Control system for three-phase active power filter which simultaneously compensates power factor and unbalanced loads," *IEEE Trans. Ind. Electron.*, Vol. 42, pp. 636–641, December 1995.
17. Ametani, A., "Harmonic reduction in thyristor converters by harmonic current injection," *IEEE Trans. Power Appl. Syst.*, Vol. PAS-95, pp. 441–449, March/April 1976.
18. Choe, G. H., and Park, M. H., "A new onjection method for AC harmonic elimination by active power filter," *IEEE Trans. Ind. Electron.*, Vol. IE-35, pp. 141–147, February 1988.
19. Williams, S. M., and Hoft, R. G., "Adaptive frequency-domain control of PWM switched power line conditioner," *IEEE Trans. Power Electron.*, Vol. 6, pp. 665–670, October 1991.
20. Driesen, J., and Belmans, R., "Active power filter control algorithms using wavelet-based power definitions," *10th Int. Conf. Harmonics Quality Power*, Vol. 2, pp. 466–471, 2002.
21. Gupta, K. K., Kumar, R., and Manjunath, H. V., "Active power filter control algorithm using wavelets," *International Conference on Power Electronics, Drives and Energy Systems (PEDES'06)*, pp. 1–4, New Delhi, India, 12–15 December 2006.
22. Liu, H., Liu, G., and Shen, Y., "Application of fast lifting wavelet transform to the estimation of harmonic for shunt active power filters," *7th International Conference on Power Electronics (ICPE '07)*, pp. 96–101, Denmark, 22–26 October 2007.
23. Gaouda, A. M., Salama, M. M. A., Sultan, M. K., and Chikhani, A. Y., "Power quality detection and classification using wavelet-multiresolution signal decomposition," *IEEE Trans. Power Delivery*, Vol. 14, No. 4, pp. 1469–1476, October 1999.
24. Stockwell, R. G., Mansinha, L., and Lowe, R. P., "Localization of the complex spectrum: The S-transform," *IEEE Trans. Signal Process.*, Vol. 44, No. 4, pp. 998–1001, April 1996.
25. Dash, P. K., Panigrahi, B. K., and Panda, G., "Power quality analysis using S-transform," *IEEE Trans. Power Delivery*, Vol. 18, No. 2, pp. 406–411, April 2003.
26. Zhao, F., and Yang, R., "Power-quality disturbance recognition using S-transform," *IEEE Trans. Power Delivery*, Vol. 22, No. 2, pp. 944–950, April 2007.
27. Assous, S., Humeau, A., Tartas, M., Abraham, P., and L'Huillier, J.-P., "S-transform applied to laser doppler flowmetry reactive hyperemia signals," *IEEE Trans. Biomed. Eng.*, Vol. 53, No. 6, pp. 1032–1037, June 2006.